Available online at www.sciencedirect.com
ScienceDirect
Lithos 98 (2007) 177–194
LITHOS
www.elsevier.com/locate/lithos

Experimental study of the joins forsterite–diopside–leucite– and forsterite–leucite–åkermanite up to 2.3 GPa [$P(H_2O)=P(Total)$] and variable temperatures: Its petrological significance

Kaustav Nag [a], Makoto Arima [b,*], Alok K. Gupta [c]

[a] *Exploration & Development Directorate, Oil and Natural Gas Corporation, Dehradun 248001, India*
[b] *Geological Institute, Graduate School of Environment and Information Sciences, Yokohama National University, 79-7, Tokiwadai, Hodogaya-ku, Yokohama 240-14 8501, Japan*
[c] *National Centre of Experimental Mineralogy and Petrology, University of Allahabad, U.P. 211002, India*

Received 28 September 2006; accepted 28 March 2007
Available online 13 April 2007

Abstract

We conducted a series of melting experiments in the join forsterite–diopside–leucite under 0.1 and 2.3 GPa and in the join forsterite–leucite–åkermanite under 2.3 GPa to understand paragenetic relationships amongst different types of lamproitic and lamprophyric magmas with K-rich mafic and ultramafic volcanic (kamafugitic) rocks. Both the joins were studied in the presence of excess water. The experimental results of the join forsterite–diopside–leucite at 0.1 GPa show that the five-phase point of forsterite $(Fo)_{ss}$ + diopside $(Di)_{ss}$ + leucite $(Lc)_{ss}$ + liquid (Liq) + vapour (V) (equivalent to ugandite lava) occurs at $Fo_2Di_{50}Lc_{48}$ at 880 ± 5 °C. Phlogopite appears as the last phase at 830 ± 15 °C. The final crystalline assemblage of $forsterite_{ss}$ + $diopside_{ss}$ + $leucite_{ss}$ + phlogopite is similar to the phenocryst assemblage of missourite lava. Present study suggests that an olivine leucitite (ugandite) can be derived from an olivine italite, a slightly potassic peridotite and a leucitite magma.

A study of the join Fo–Di–Lc [$P(H_2O)=P(Total)$] at 2.3 GPa shows that liquid compositions penetrate the primary phase volumes of $forsterite_{ss}$, $phlogopite_{ss}$, kalsilitess, K-$feldspar_{ss}$ and $diopside_{ss}$. It has the following three five-phase points: 1) one occurring at $Fo_9Di_{49}Lc_{42}$ and 1005 ± 5 °C, where liquid and vapour coexists with $forsterite_{ss}$, $phlogopite_{ss}$ and $diopside_{ss}$ (phlogopite-bearing madupite), 2) the second one at $Fo_4Di_{50}Lc_{46}$ and 990 ± 10 °C, where $diopside_{ss}$, K-$feldspar_{ss}$ and $phlogopite_{ss}$ coexist with liquid and vapour (pyroxene-bearing minette), and 3) the third one at $Fo_3Di_{21}Lc_{76}$ and 775 ± 5 °C, where $phlogopite_{ss}$, $kalsilite_{ss}$ and K-$feldspar_{ss}$ are in equilibrium with liquid plus vapour (kalsilite-bearing minette).

The experimental results of the join Fo–Lc–åkermanite (Ak) show that the join 40 penetrates the primary phase volumes of $forsterite_{ss}$, $phlogopite_{ss}$, kalsilite, K-$feldspar_{ss}$, $diopside_{ss}$ and $merwinite_{ss}$. The data indicate the presence of four five-phase points: 1) one occurring at $Fo_7Lc_{42}Ak_{51}$ and 1165 ± 5 °C, where $phlogopite_{ss}$, $forsterite_{ss}$, $diopside_{ss}$ coexists with liquid and vapour (olivine-bearing madupite), 2) the second one at $Fo_3Lc_{49}Ak_{48}$ and 1140 ± 10 °C, where a liquid is in equilibrium with $phlogopite_{ss}$, K-$feldspar_{ss}$, $diopside_{ss}$ and vapour (pyroxene-bearing minette), 3) the third one at $Fo_{18}Lc_{21}Ak_{61}$ and 1255 ± 10 °C, where $merwinite_{ss}$, $forsterite_{ss}$ and $diopside_{ss}$ are in equilibrium with liquid and vapour (merwinite-bearing wherlite), and 4) the fourth one at $Fo_5Lc_{73.5}Ak_{21.5}$ and 770 ± 5 °C, where $kalsilite_{ss}$, $phlogopite_{ss}$ and K-feldspar coexist with liquid and vapour (kalsilite-bearing

* Corresponding author. Geological Institute, Yokohama National University, 156, Tokiwadai, Hodogaya-ku, Yokohama 240, Japan. Tel.: +81 45 339 3354; fax: +81 45 339 3264.
E-mail address: arima@ed.ynu.ac.jp (M. Arima).

0024-4937/$ - see front matter © 2007 Elsevier B.V. All rights reserved.
doi:10.1016/j.lithos.2007.03.006

minette). The present data suggest that high pressure heteromorphic equivalent of a katungite magma is represented by a kalsilite-bearing minette, a pyroxene-bearing minette, or an olivine-bearing madupite.
© 2007 Elsevier B.V. All rights reserved.

Keywords: Ultrapotassic rocks; High-pressure melting phase relationships; Forsterite–leucite–diopside join; Forsterite–leucite–åkermanite join; Kamafugitic rocks

1. Introduction

The four essential minerals of many high-K mafic and ultramafic igneous (kamafugitic) rocks are leucite, augite, olivine, and melilite. The bulk rock compositions of these rocks lie within the phase volume of Fo–Di–Lc–Ak and melting phase relationships of this system is thus applicable to the understanding of the origin of high-K mafic and ultramafic igneous rocks (Yoder, 1986). The phase volume of Fo–Di–Lc–Ak is a part of the larnite–forsterite–kalsilite–silica tetrahedron (Fig. 1). Phase equilibria in this larnite-based basaltic tetrahedron have been studied for last several decades at atmospheric pressure (Schairer and Bowen, 1938; Luth, 1967; Gupta, 1972; Yoder, 1986; Veksler et al., 1998).

Phlogopite is the most abundant hydrous liquidus mineral in high-K mafic and ultramafic igneous rocks and much attention has been paid to the melting phase relationships of phlogopite-bearing mafic and ultramafic igneous rocks (ex. Barton and Hamilton, 1979; Arima and Edgar, 1983a,b; Foley et al., 1987; Foley, 1992; Gupta et al., 2002; Conceicaoção and Green, 2004). The high pressure melting experimental studies have been conducted in the join forsterite–kalsilite–quartz at different P–T conditions and in the presence of several volatile components (H_2O, CO_2, F) (Modreski and Boettcher, 1973; Wendlandt and Eggler, 1980a,b; Wendlandt, 1984: Foley et al., 1986: Gupta and Green, 1988; Melzer and Foley, 1996). Recently, Conceicaoção and Green (2000) added silica to the forsterite–leucite join to elucidate the genesis of K-rich silica-saturated magmas from lherzolitic source rocks.

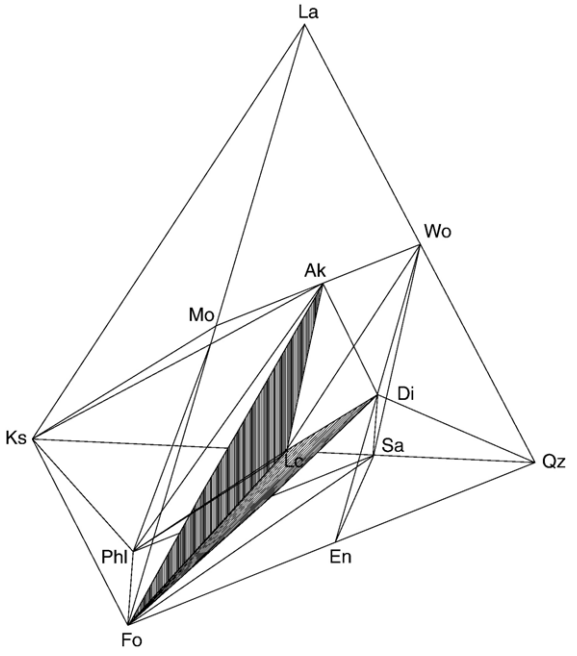


Fig. 1. The joins Fo–Di–Lc and Fo–Lc–Ak as a part of the La–Fo–Ks–Qz tetrahedron (after Yoder, 1986). Abbreviations are given in text.

In the present study, we have added diopside or åkermanite to the forsterite–leucite join to understand the heteromorphic relationship between the K-rich mafic and ultramafic volcanic rocks with lamprophyric or lamproitic melts originated in the upper mantle. In either of these two joins, leucite is expected to break down at high pressures and temperatures by the following reaction (Scarf et al., 1966; Fasshauer et al., 1998);

$$2\mathrm{Lc} = \mathrm{K-feldspar(Kf)} + \mathrm{kalsilite(Ks)} \quad (1)$$

In cases of both the joins Fo–Di–Lc and Fo–Lc–Ak under a condition of 2.3 GPa [$P(H_2O)=P(\mathrm{Total})$], phlogopite is an additional phase and forsterite reacts with leucite to produce the following assemblage typical of minette (Yoder, 1986):

$$3\mathrm{Fo} + 2\mathrm{Lc} + 2H_2O = 2\mathrm{Ph} + \mathrm{Kf} \quad (2)$$

The above discussion suggests that in the join Fo–Di–Lc at elevated pressures and temperatures, various combinations of phlogopite$_{ss}$, diopside$_{ss}$, kalsilite$_{ss}$, forsterite$_{ss}$ and K-feldspar$_{ss}$ may appear. Such assemblages are typical of lamproitic and lamprophyric rocks (Gupta and Yagi, 1980; Foley et al., 1987; Rock, 1991; Mitchell and Bergman, 1991).

In case of the join Fo–Lc–Ak following reactions are also expected under high pressures (Yoder, 1973, 1986):

$$2\mathrm{Ak} + \mathrm{Fo} + 3\mathrm{Lc} = 4\ \mathrm{clinopyroxene(Cpx)} + 3\mathrm{Ks} \quad (3)$$

$$2\mathrm{Ak} = \mathrm{Di} + \mathrm{merwinite(Mer)} \quad (4)$$

$$\mathrm{Ak} + 5\mathrm{Fo} + 3\mathrm{Lc} + 3H_2O = 3\mathrm{Ph} + 2\mathrm{Cpx} \quad (5)$$

In the join Fo–Lc–Ak, reactions (2), (3), (4) and (5) lead to various assemblages found in lamprophyres and lamproitic rocks, and melting relationships in the join Fo–Lc–Ak have therefore, significant bearing on their genesis.

2. Experimental techniques

A hydrothermal cold seal externally heated apparatus (Model HR-IB-2) was used to conduct experiments at 0.1 GPa [($P(H_2O)=P$(Total)] at the National Centre of Experimental Mineralogy and Petrology, Allahabad. All experiments at 2.3 GPa were performed using a piston-cylinder apparatus (Boyd and England, 1960) at the same Centre. Talc-pyrex cell assemblies (diameter: 12.7 mm, length: 43.7 mm) were used for runs with a piston-cylinder apparatus. Measurement of temperatures was made with Pt–$Pt_{87}Rh_{13}$ thermocouples and is considered to br accurate to ±5 °C without taking into account the effect of pressure on e.m.f. Pressure was calibrated at 1000 °C against the reactions fayalite = magnetite + quartz (1.41 GPa; Bohlen et al., 1980) and quartz = coesite (3.07 GPa; Bose and Ganguly, 1995). We wished to conduct all experiments at 2 GPa, but pressure calibration indicated that the runs were in effect performed under 2.3 GPa. Pressure measurements are considered to be accurate to ± 0.05 GPa. Originally the pressure of 2 GPa was chosen so that results can be compared with those of Wendlandt and Eggler (1980a), who studied the join kalsilite–forsterite–silica with or without volatiles at 2 GPa and different temperatures.

Reagent grade $CaCO_3$, MgO, Al_2O_3, and K_2CO_3 were used as sources of CaO, MgO, Al_2O_3, and K_2O, respectively. Pure quartz (99.9%) collected from Matheran, Maharastra was used as a source of silica. Magnesia and Al_2O_3 were heated in a furnace for 1 h at 800 °C to remove water present either as $Mg(OH)_2$ or $Al_2O_3 \cdot nH_2O$. For the preparation of glass, actual ingredients were mechanically mixed after carefully weighing them in a microbalance and mixing them with acetone in an agate mortar for an hour. The mixtures were then fused to glasses. Schairer's (1950) method of preparation of glass and crystallization of starting materials was adopted. All glasses were crystallized at 1 atmospheric pressure and 800 °C for about 5 days. The high pressure runs were then conducted on these crystallized starting materials. To facilitate nucleation and crystal growth, the materials were crushed in an agate mortar with acetone everyday till crystallization was complete. The refractive indices of all the glasses were measured to check the homogeneity. In case of two compositions $forsterite_5diopside_{45}leucite_{50}$ and $forsterite_3diopside_{60}leucite_{37}$, glasses could not be made because of high liquidus temperatures. These two compositions were sintered at 1400 °C twice for 1 h. Hence, homogeneous sintered materials were used for experimental runs. In our experiments 20 wt.% water was always added to the samples contained in a capsule, the bottom end of which was already fused. The tube containing the sample and water was wrapped with wet cotton, crimped at the top and welded with a graphite arc welder. After the welding the tube along with sample and water was placed in an oven. The temperature of the oven was maintained at 110 °C for several hours. The dried capsule was once again weighed to ensure that there was no loss of water. The experiments were done invariably in presence of 20 wt.% water. After the experiment was over the samples were cleaned with acetone and weighed again. When the tube was cut open we observed the presence of excess water. Identification of phases was made using a microscope provided by M/s James Swift Co. U.K, and by an X-ray diffractometer obtained from the Seifert Company. The phases were analyzed by using Cameca EPMA (accelerating voltage 15 kV, sample current 25 nA) at the University of Bristol, U.K. and with SEM-EDS (Link QX2000) at the Yokohama National University, Japan. While analyzing the glass with the electron beam of an EMPA, volatilization of water present in the glass could be observed. Presence of minute water bubbles could also be seen within the glasses containing different phases.

Following abbreviations have been used in the text, tables and figures to describe compositions and phases: En: enstatite, Fo: forsterite, Ak: åkermanite. La: larnite, Lc: leucite, Ks: kalsilite, Ol: olivine, Ph: phlogopite, Kf: K-feldspar, Di: diopside, La: Mer: merwinite, Mo: monticellite, Qz: quartz, Sa: sanidine, Wo: wollastonite, Gl: glass, Liq: liquid, V: vapour, f: fluid, and ss: solid solution.

3. Experimental results

3.1. Phases

The run results are listed in Table 1 for the join Fo–Di–Lc at 0.1 GPa, in Table 2 for the join Fo–Di–Lc at 2.3 GPa, and in Table 3 for the join Fo–Lc–Ak at 2.3 GPa.

A series of reversal runs were conducted. In the join Fo–Di–Lc at 0.1 GPa, the run A22 equilibrated at 850 °C and 0.1 GPa was reversed at 865 °C (compare run A23 and run A24 marked 'r' in Table 1. Like wise, the run no. A33 equilibrated at 850 °C was reversed at 870°C (run A34) and 900°C (run A35). Compare the

Table 1
Experimental runs on the join Fo–Di–Lc at 0.1 GPa

Run no.	Mixture no.	Composition	Temperature (°C)	Duration (h)	Assemblage
A1	FDL-1	$Fo_{10}Di_{45}Lc_{45}$	900	1	Fo+Gl+V
A2	FDL-1	$Fo_{10}Di_{45}Lc_{45}$	875	60	Fo>Di>Lc+Gl+V
A4	FDL-1	$Fo_{10}Di_{45}Lc_{45}$	830	50	Fo>Di>Lc>Ph+Gl+V
A5	FDL-1	$Fo_{10}Di_{45}Lc_{45}$	800	90	Fo>Di>Lc>Ph+Gl+V
A6	FDL-2	$Fo_{10}Di_{55}Lc_{35}$	900	1	Fo+Gl+V
A7	FDL-2	$Fo_{10}Di_{55}Lc_{35}$	875	2	Fo>Di=Lc Gl+V
A8	FDL-2	$Fo_{10}Di_{55}Lc_{35}$	850	150	Fo>Di=Lc+Gl+V
A9	FDL-2	$Fo_{10}Di_{55}Lc_{35}$	800	90	Fo>Di>Lc>Ph+Gl+V
A10	FDL-3	$Fo_{10}Di_{65}Lc_{25}$	890	3	Fo>Di+Gl+V
A11	FDL-3	$Fo_{10}Di_{65}Lc_{25}$	850	150	Fo>Di>Lc+Gl+V
A12	FDL-3	$Fo_{10}Di_{65}Lc_{25}$	875	2	Fo>Di=Lc+Gl+V
A13	FDL-4	$Fo_5Di_{55}Lc_{40}$	900	1	Gl+V
A14	FDL-4	$Fo_5Di_{55}Lc_{40}$	875	2	Di=Fo>Lc+Gl+V
A15	FDL-4	$Fo_5Di_{55}Lc_{40}$	850	150	Di>Fo>Lc+Gl+V
A16	FDL-4	$Fo_5Di_{55}Lc_{40}$	800	90	Fo>Lc>Di>Ph+Gl+V
A17	FDL-5	$Fo_5Di_{65}Lc_{30}$	900	1	Gl+V
A18	FDL-5	$Fo_5Di_{65}Lc_{30}$	885	2	Di>Fo+Gl+V
A19	FDL-5	$Fo_5Di_{65}Lc_{30}$	875	2	Di>Fo≫Lc+Gl+V
A20	FDL-5	$Fo_5Di_{65}Lc_{30}$	850	2	Di>Fo>Lc+Gl+V
A21	FDL-6	$Fo_5Di_{45}Lc_{50}$	900	1	Gl+V
A22[a]	FDL-6	$Fo_5Di_{45}Lc_{50}$	850	150	Fo>Lc>Di+Gl+V
A23	FDL-6	$Fo_5Di_{45}Lc_{50}$	865	5	Fo>Lc>Gl+V
A24(r)	FDL-6	$Fo_5Di_{45}Lc_{50}$	865	2	Fo>Lc>Gl+V
A25	FDL-6	$Fo_5Di_{45}Lc_{50}$	880	2	Fo+Gl+V
A26	FDL-6	$Fo_5Di_{45}Lc_{50}$	800	90	Fo>L>Di>Ph+Gl+V
A27	FDL-7	$Fo_4Di_{48}Lc_{48}$	890	3	Gl+V
A28	FDL-7	$Fo_4Di_{48}Lc_{48}$	870	2	Fo>Di=Lc+Gl+V
A29	FDL-8	$Fo_5Di_{40}Lc_{55}$	880	5	Gl+V
A30	FDL-8	$Fo_5Di_{40}Lc_{55}$	870	6	Fo>Di+Gl+V
A31	FDL-9	$Fo_3Di_{40}Lc_{57}$	900	147	Lc>Di+Gl+V
A32	FDL-9	$Fo_3Di_{40}Lc_{57}$	870	150	Lc>Di>Fo+Gl+V
A33[a]	FDL-9	$Fo_3Di_{40}Lc_{57}$	850	76	Fo≫Lc>Di+Gl+V
A34(r)	FDL-9	$Fo_3Di_{40}Lc_{57}$	870	50	Lc>Di>Fo+Gl+V
A35(r)	FDL-9	$Fo_3Di_{40}Lc_{57}$	900	2	Lc>Di+Gl+V
A36	FDL-21	$Fo_{15}Di_{79}Lc_6$	910	2	Gl+V
A37	FDL-21	$Fo_{15}Di_{79}Lc_6$	900	2	Fo+Gl+V
A38	FDL-22	$Fo_{12}Di_{80}Lc_8$	900	2	Gl+V
A39	FDL-22	$Fo_{12}Di_{80}Lc_8$	890	2	Di+Gl+V
A40	FDL-23	$Di_{60}Lc_{40}$	900	1	Gl+V
A41	FDL-23	$Di_{60}Lc_{40}$	885	2	Di>Lc+Gl+V
A42	FDL-24	$Di_{55}Lc_{45}$	890	3	Gl+V
A43	FDL-24	$Di_{55}Lc_{45}$	882	3	Di>Lc+Gl+V
A44	FDL-25	$Di_{47}Lc_{53}$	890	1	Lc>Di+Gl+V
A45	FDL-26	$Di_{48.5}Lc_{51.5}$	890	1	Lc>Di+Gl+V
A46	FDL-27	$Di_{15}Di_{40}Lc_{45}$	920	30	Fo>Gl+V
A47	FDL-27	$Di_{15}Di_{40}Lc_{45}$	890	24	Fo>Lc>Gl+V
A48	FDL-27	$Di_{15}Di_{40}Lc_{45}$	880	30	Fo>Lc>Di+Gl+V

All assemblages contained an additional vapour phase. The symbols ≫, > etc indicate relative proportion of the phases. Abbreviations are same as those mentioned in the text.

[a] Run (A22) was repeated at 865 °C (A24) to see if it is similar to run A23. Similarly run product (A33) was rerun at 870 °C (A34) and 900 °C (A35) to see if they are similar to runs A32 and A31. Runs reversed at lower temperature are indicated by letter (r).

runs A34 and A35 marked 'r' with those of A32 and A31. The results were same in both sets of runs. In the join Fo–Di–Lc at 2.3 GPa, an experimental charge (run B57) conducted at 750 °C and 2.3 GPa was reversed at 770 °C (run B58) and 780 °C (run B59) (Table 2). Compare the runs B58 and B59 with those of B56 and B55. The results were same in both sets of runs. In the join Fo–Lc–Ak at 2.3 GPa (Table 3), the composition

Table 2
Experimental run products in the join Fo–Di–Lc at 2.3 GPa

Run no.	Mixture no.	Composition	Temperature (°C)	Duration (h)	Assemblage
B1	FDL-1	$Fo_{10}Di_{45}Lc_{45}$	1150	3	Gl+V
B2	FDL-1	$Fo_{10}Di_{45}Lc_{45}$	1100	4	Gl+V
B3	FDL-1	$Fo_{10}Di_{45}Lc_{45}$	1050	5	Gl+V
B4	FDL-1	$Fo_{10}Di_{45}Lc_{45}$	1025	5	Gl+V
B5	FDL-1	$Fo_{10}Di_{45}Lc_{45}$	1005	5	Fo>Ph>Di+Gl+V
B6	FDL-2	$Fo_{10}Di_{55}Lc_{35}$	1150	3.5	Gl+V
B7	FDL-2	$Fo_{10}Di_{55}Lc_{35}$	1100	5	Gl+V
B8	FDL-2	$Fo_{10}Di_{55}Lc_{35}$	1075	5	Gl+V
B9	FDL-2	$Fo_{10}Di_{55}Lc_{35}$	1025	5	Gl+V
B10	FDL-2	$Fo_{10}Di_{55}Lc_{35}$	1005	6	Fo>Di>Ph+Gl+V
B11	FDL-2	$Fo_{10}Di_{55}Lc_{35}$	975	6	Fo>Di>Ph>Kf+Gl+V
B12	FDL-3	$Fo_{10}Di_{65}Lc_{25}$	1150	4	Gl+V
B13	FDL-3	$Fo_{10}Di_{65}Lc_{25}$	1100	4	Gl+V
B14	FDL-3	$Fo_{10}Di_{65}Lc_{25}$	1025	6	Gl+V
B15	FDL-3	$Fo_{10}Di_{65}Lc_{25}$	1005	6	Fo=Di>Ph+Gl+V
B16	FDL-3	$Fo_{10}Di_{65}Lc_{25}$	970	6	Fo=Di>Ph>Kf+Gl+V
B17	FDL-4	$Fo_5Di_{55}Lc_{40}$	1150	4	Gl+V
B18	FDL-4	$Fo_5Di_{55}Lc_{40}$	1075	5	Gl+V
B19	FDL-4	$Fo_5Di_{55}Lc_{40}$	1025	5	Gl+V
B20	FDL-4	$Fo_5Di_{55}Lc_{40}$	1010	5	Di+Gl+V
B21	FDL-4	$Fo_5Di_{55}Lc_{40}$	1005	6	Di>Ph=Fo+Gl+V
B22	FDL-4	$Fo_5Di_{55}Lc_{40}$	950	6	Di>Ph>Fo>Kf+Gl+V
B23	FDL-5	$Fo_5Di_{65}Lc_{30}$	1150	4	Gl+V
B24	FDL-5	$Fo_5Di_{65}Lc_{30}$	1100	5	Gl+V
B25	FDL-5	$Fo_5Di_{65}Lc_{30}$	1025	5	Di+Gl+V
B26	FDL-5	$Fo_5Di_{65}Lc_{30}$	1005	6	Di>Ph>Fo+Gl+V
B27	FDL-5	$Fo_5Di_{65}Lc_{30}$	975	6	Di>Ph>Fo>Kf+Gl+V
B28	FDL-6	$Fo_5Di_{45}Lc_{50}$	1150	4	Gl+V
B29	FDL-6	$Fo_5Di_{45}Lc_{50}$	1100	4	Gl+V
B30	FDL-6	$Fo_5Di_{45}Lc_{50}$	1025	6	Ph+Gl+V
B31	FDL-6	$Fo_5Di_{45}Lc_{50}$	1000	7	Ph>Di+Gl+V
B32	FDL-6	$Fo_5Di_{45}Lc_{50}$	980	6	Ph>Di>Kf+Gl+V
B33	FDL-9	$Fo_3Di_{40}Lc_{57}$	1200	2	Gl+V
B34	FDL-9	$Fo_3Di_{40}Lc_{57}$	1150	2	Gl+V
B35	FDL-9	$Fo_3Di_{40}Lc_{57}$	900	2	Gl+V
B36	FDL-9	$Fo_3Di_{40}Lc_{57}$	850	6	Kf>Ph+Gl+V
B37	FDL-9	$Fo_3Di_{40}Lc_{57}$	805	2	Kf>Ph>Di+Gl+V
B38	FDL-10	$Fo_3Di_{50}Lc_{47}$	1200	2	Gl+V
B39	FDL-10	$Fo_3Di_{50}Lc_{47}$	1150	3	Gl+V
B40	FDL-10	$Fo_3Di_{50}Lc_{47}$	1000	2.5	Kf=Ph+Gl+V
B41	FDL-10	$Fo_3Di_{50}Lc_{47}$	990	5	Kf=Ph>Di+Gl+V
B42	FDL-11	$Fo_3Di_{60}Lc_{37}$	1200	2	Gl+V
B43	FDL-11	$Fo_3Di_{60}Lc_{37}$	1150	2	Gl+V
B44	FDL-11	$Fo_3Di_{60}Lc_{37}$	1010	5	Di+Gl+V
B45	FDL-11	$Fo_3Di_{60}Lc_{37}$	990	5	Di>Kf>Ph+Gl+V
B46	FDL-12	$Di_{40}Lc_{60}$	970	5	Gl+V
B47	FDL-12	$Di_{40}Lc_{60}$	950	4	Kf>Di+Gl+V
B48	FDL-13	$Lc_{30}Di_{70}$	1050	4	Di>Kf+Gl+V
B49	FDL-14	$Fo_{15}Di_{15}Lc_{70}$	1150	4	Ph>Fo+Gl+V
B50	FDL-15	$Lc_{70}Di_{30}$	800	2	Kf+Gl+V
B51	FDL-16	$Lc_{85}Di_{15}$	800	2	Ks>Kf+Gl+V
B52	FDL-17	$Lc_{77.5}Di_{22.5}$	800	3	Kf>Ks+Gl+V
B53	FDL-17	$Lc_{77.5}Di_{22.5}$	780	3	Kf>Ks+Gl+V
B54	FDL-18	$Fo_5Di_{15}Lc_{80}$	775	3	Ph>Ks>Kf+Gl+V
B55	FDL-19	$Fo_5Di_{20}Lc_{75}$	780	5	Gl+V
B56	FDL-19	$Fo_5Di_{20}Lc_{75}$	770	5	Ph>Ks=Kf>Di+Gl+V
B57[a]	FDL-19	$Fo_5Di_{20}Lc_{75}$	750	4	Ph>Ks=Kf>Di+Gl+V

(continued on next page)

Table 2 (*continued*)

Run no.	Mixture no.	Composition	Temperature (°C)	Duration (h)	Assemblage
B58(r)	FDL-19	$Fo_5Di_{20}Lc_{75}$	770	7	Ph>Ks>Kf+Gl+V
B59(r)	FDL-19	$Fo_5Di_{20}Lc_{75}$	780	5	Gl+V
B60	FDL-20	$Fo_{20}Di_{30}Lc_{50}$	1210	2	Fo+Gl+V
B61	FDL-20	$Fo_{20}Di_{30}Lc_{50}$	1150	4	Fo>Ph+Gl+V
B62	FDL-20	$Fo_{20}Di_{30}Lc_{50}$	1005	4	Fo>Ph>Di+Gl+V
B63	FDL-20	$Fo_{20}Di_{30}Lc_{50}$	985	5	Fo>Ph>Di>Kf+Gl+V
B64	FDL-21	$Fo_{10}Lc_{90}$	980	5	Ph>Ks+Gl+V
B65	FDL-21	$Fo_{10}Lc_{90}$	1000	4	Gl+V
B66	FDL-22	$Fo_{20}Di_{30}Lc_{50}$	1230	1	Fo+Gl+V
B67	FDL-22	$Fo_{20}Di_{30}Lc_{50}$	1110	2	Fo>Ph+Gl+V
B68	FDL-22	$Fo_{20}Di_{30}Lc_{50}$	1020	4	Ph>Fo>+Gl+V
B69	FDL-22	$Fo_{20}Di_{30}Lc_{50}$	1005	1	Fo>Ph>Di+Gl+V
B70	FDL-23	$Fo_{2.5}Di_{60}Lc_{37.5}$	1010	1	Di+Gl+V
B71	FDL-23	$Fo_{2.5}Di_{60}Lc_{37.5}$	1005	2	Di>Kf+Gl+V
B71	FDL-23	$Fo_{2.5}Di_{60}Lc_{37.5}$	990	1	Di>Kf>Ph+Gl+V

All assemblages contained an additional vapour phase. The symbols ≫, > etc indicate relative proportion of the phases. Abbreviations are same as those mentioned in the text.

[a] Run (B57) crystallized at 750 °C was re-run at 770 °C (B58) and 780 °C (B59) to see if it is similar to run B56 and B55, respectively. Runs reversed at lower temperature are indicated by letter (r).

($Fo_5Ak_{20}Lc_{75}$) crystallized at 750 °C and 2.3 GPa (run C58), was reversed at 780 and 800 °C (compare run no. C59 and C60 marked 'r' with C57 and C56). The results in both sets of runs are identical. These data suggest that equilibrium condition was achieved in our experimental runs.

The crystalline phases obtained in the study of the join Fo–Di–Lc at 0.1 GPa [$P(H_2O)=P$(Total)] and variable temperatures include leucite, forsterite, diopside and phlogopite. The phases appearing in the same join at 2.3 GPa comprise phlogopite, kalsilite, K-feldspar, forsterite and diopside. In the join Fo–Lc–Ak following phases were obtained: forsterite, diopside, phlogopite, kalsilite, K-feldspar and merwinite.

Compositions of some of the glasses in equilibrium with crystalline phases are given in Table 4. Glasses obtained above the liquidus temperatures are also listed, which are similar to the theoretical compositions of starting materials (Table 4). The glasses present in all the run products contain a vapour phase in the form of minute globules. The electron microprobe analyses of forsterite (Table 5), diopside (Table 5), phlogopite (Table 6), leucite (Table 6), K-feldspar (Table 7), kalsilite (Table 7) and merwinite (Table 7) suggest that except for kalsilite all other crystalline phases appearing in the present study are solid solutions. The kalsilites analyzed are nearly of stoichiometric composition.

Forsterite occurs as euhedral prisms at or near liquidus conditions with straight extinction, but at low temperatures it is rounded or stubby crystals with parallel extinction with respect to the elongation direction. Warner and Luth (1973) established that the amount of monticellite content in olivine should not exceed 1% CaO under mantle pressure condition. The CaO content of forsterite equilibrated in the joins Fo–Di–Lc and Fo–Lc–Ak at 2.3 GPa from various compositions range between 0.01 and 0.26 wt.% (Table 5).

Diopside occurs as stout prisms with inclined extinction (Z Γ C=38–42°) near the liquidus. It has slightly higher birefringence than that of forsterite. Microprobe analyses of diopside crystallized from different compositions (Table 5) shows that it contains 1.35 to 6.18 wt.% Al_2O_3, which corresponds to 7 to 24 wt.% $CaAl_2SiO_6$ molecule. The diopside crystallized in the join Fo–Lc–Ak contains 4.04 to 5.01 wt.% Al_2O_3, as $CaAl_2SiO_6$ molecule.

Phlogopite occurs as hexagonal grains near the liquidus but it appears as needle-shaped or rounded grains at lower temperatures. X-ray diffraction patterns of phlogopite suggest the presence of 1 M or 3T polytype. Table 6 shows that phlogopite has variable compositions in that Al^{3+} is found to replace Si^{4+} in the tetrahedral site. Likewise, Mg^{2+} in the octahedral site is substituted by Al^{3+} and to maintain electrical neutrality Si^{4+} is replaced by Al^{3+} in the four coordinated site. Substitution by $Mg^{2+}=Al^{3+}$ and $Si^{4+}=Al^{3+}$ might have taken place in the octahedral and tetrahedral sites.

Leucite (Table 6) appears as an isotropic crystal (N=1.508) with eight-sided outline only in the join Fo–Di–Lc studied under 0.1 GPa [$P(H_2O)=P$(Total)]. It is absent in the same join or in the join Fo–Lc–Ak investigated at 2.3 GPa.

K-feldspar occurs as small plates but elongated crystals or needles are also common. It contains minor amount of

Table 3
Experimental run products in the join Fo–Lc–Ak at 2.3 GPa

Run no.	Mixture no.	Composition	Temperature (°C)	Duration (h)	Assemblage
C1	FLA-1	$Fo_{10}Lc_{45}Ak_{45}$	1250	2	Gl+V
C2	FLA-1	$Fo_{10}Lc_{45}Ak_{45}$	1240	2	Gl+V
C3	FLA-1	$Fo_{10}Lc_{45}Ak_{45}$	1230	2	Fo>Ph+Gl+V
C4	FLA-1	$Fo_{10}Lc_{45}Ak_{45}$	1175	2	Fo>Ph+Gl+V
C5	FLA-1	$Fo_{10}Lc_{45}Ak_{45}$	1150	3	Fo>Di+Ph+Gl+V
C6	FLA-2	$Fo_{10}Lc_{55}Ak_{35}$	1250	2.5	Gl+V
C7	FLA-2	$Fo_{10}Lc_{55}Ak_{35}$	1240	3	Fo+Gl+V
C8	FLA-2	$Fo_{10}Lc_{55}Ak_{35}$	1200	3	Ph>Fo+Gl+V
C9	FLA-2	$Fo_{10}Lc_{55}Ak_{35}$	1150	5	Ph>Fo>Di+Gl+V
C10	FLA-2	$Fo_{10}Lc_{55}Ak_{35}$	1100	5	Ph>Fo>Di+Kf+V
C11	FLA-3	$Fo_{5}Lc_{55}Ak_{40}$	1250	1	Gl+V
C12	FLA-3	$Fo_{5}Lc_{55}Ak_{40}$	1240	3	Ph+Gl+V
C13	FLA-3	$Fo_{5}Lc_{55}Ak_{40}$	1200	2	Ph>Kf+Gl+V
C14	FLA-3	$Fo_{5}Lc_{55}Ak_{40}$	1150	5	Ph>Kf+Gl+V
C15	FLA-3	$Fo_{5}Lc_{55}Ak_{40}$	1130	5	Ph>Kf=Di+Gl+V
C16	FLA-4	$Fo_{15}Lc_{5}Ak_{80}$	1270	4.5	Gl+V
C17	FLA-4	$Fo_{15}Lc_{5}Ak_{80}$	1260	2	Mer>Fo+Gl+V
C18	FLA-4	$Fo_{15}Lc_{5}Ak_{80}$	1250	2	Mer>Fo>Di+Gl+V
C19	FLA-4	$Fo_{15}Lc_{5}Ak_{80}$	1200	1	Fo≫Di>Mer+Gl+V
C20	FLA-4	$Fo_{15}Lc_{5}Ak_{80}$	1100	5	Fo>Di>Ph>Kf+Gl+V
C21	FLA-5	$Fo_{15}Lc_{10}Ak_{75}$	1380	3	Gl+V
C22	FLA-6	$Fo_{15}Lc_{10}Ak_{75}$	1250	1	Mer>Di>Fo+Gl+V
C23	FLA-7	$Fo_{10}Lc_{30}Ak_{60}$	1240	2	Gl+V
C24	FLA-7	$Fo_{10}Lc_{30}Ak_{60}$	1230	5	Di+Fo+Gl+V
C25	FLA-8	$Fo_{10}Lc_{20}Ak_{70}$	1260	4	Gl+V
C26	FLA-8	$Fo_{10}Lc_{20}Ak_{70}$	1250	2	Mer>Di+Gl+V
C27	FLA-9	$Fo_{20}Ak_{80}$	1300	2	Mer≫Fo+Gl+V
C28	FLA-9	$Fo_{20}Ak_{80}$	1320	2	Mer+Gl+V
C29	FLA-10	$Fo_{15}Lc_{25}Ak_{60}$	1280	2	Ph+Gl+V
C30	FLA-10	$Fo_{15}Lc_{25}Ak_{60}$	1300	2	Gl+V
C31	FLA-10	$Fo_{15}Lc_{25}Ak_{60}$	1270	3	Ph>Fo+Gl+V
C32	FLA-11	$Fo_{7}Lc_{51}Ak_{42}$	1180	3	Gl+V
C33	FLA-11	$Fo_{7}Lc_{51}Ak_{42}$	1160	3	Fo=Di=Ph+Gl+V
C34	FLA-12	$Fo_{3}Ak_{97}$	1300	1	Mer>Di+Gl+V
C35	FLA-13	$Fo_{25}Ak_{75}$	1300	2	Fo>Mer+Gl+V
C36	FLA-14	$Lc_{77.5}Ak_{22.5}$	800	2.5	Gl+V
C37	FLA-14	$Lc_{77.5}Ak_{22.5}$	775	3	Ks>Kf+Gl+V
C38	FLA-14	$Lc_{77.5}Ak_{22.5}$	750	6	Ks>Kf>Di+Gl+V
C39	FLA-15	$Lc_{30}Ak_{70}$	1275	1	Di+Gl+V
C40	FLA-16	$Lc_{15}Ak_{85}$	1300	2	Mer>Di+Gl+V
C41	FLA-17	$Lc_{50}Ak_{50}$	1180	2.25	Gl+V
C42	FLA-17	$Lc_{50}Ak_{50}$	1170	4.5	Di>Kf+Gl+V
C43	FLA-17	$Lc_{50}Ak_{50}$	1150	5	Di>Kf+Gl+V
C44	FLA-17	$Lc_{50}Ak_{50}$	1130	5	Di>Kf>Ks+Gl+V
C45	FLA-18	$Fo_{5}Lc_{75}Ak_{20}$	800	4	Gl+V
C46	FLA-18	$Fo_{5}Lc_{75}Ak_{20}$	775	4	Ph>Ks+Gl+V
C47	FLA-18	$Fo_{5}Lc_{75}Ak_{20}$	750	4	Ph>Ks>Kf+Gl+V
C48	FLA-19	$Fo_{5}Lc_{48}Ak_{47}$	1160	1	Ph+Gl+V
C49	FLA-19	$Fo_{5}Lc_{48}Ak_{47}$	1140	5	Ph>Di=Kf+Gl+V
C50	FLA-19	$Fo_{5}Lc_{48}Ak_{47}$	1150	5	Fo+Gl+V
C51	FLA-20	$Fo_{5}Lc_{40}Ak_{55}$	1160	2	Di+Gl+V
C52	FLA-20	$Fo_{5}Lc_{40}Ak_{55}$	1150	2	Di>Fo=Ph+Gl+V
C53	FLA-21	$Lc_{85}Ak_{15}$	850	2	Gl+V
C54	FLA-21	$Lc_{85}Ak_{15}$	800	2	Ks+Gl+V
C55	FLA-21	$Lc_{85}Ak_{15}$	790	2	Ks>Kf+Gl+V
C56	FLA-22	$Fo_{5}Lc_{75}Ak_{20}$	800	2	Ks>Ph+Gl+V
C57	FLA-22	$Fo_{5}Lc_{75}Ak_{20}$	780	2	Ks>Ph>Kf+Gl+V

(continued on next page)

Table 3 (*continued*)

Run no.	Mixture no.	Composition	Temperature (°C)	Duration (h)	Assemblage
C58[a]	FLA-22	$Fo_5Lc_{75}Ak_{20}$	750	2	Ks>Ph>Kf>Di+Gl+V
C59(r)	FLA-22	$Fo_5Lc_{75}Ak_{20}$	780	2	Ks>Ph>Kf+Gl+V
C60(r)	FLA-22	$Fo_5Lc_{75}Ak_{20}$	800	6	Ks>Ph+Gl+V
C61	FLA-22	$Fo_5Lc_{75}Ak_{20}$	820	2	Gl+V
C62	FLA-23	$Fo_3Lc_{49}Ak_{48}$	1160	4	Gl+V
C63	FLA-23	$Fo_3Lc_{49}Ak_{48}$	1150	4	Ph>Fo=Kf+Gl+V
C64	FLA-24	$Fo_{15}Lc_{40}Ak_{45}$	1265	1	Fo+Gl+V
C65	FLA-24	$Fo_{15}Lc_{40}Ak_{45}$	1180	4	Fo>Ph+Gl+V
C66	FLA-24	$Fo_{15}Lc_{40}Ak_{45}$	1165	3	Fo>Ph>Di+Gl+V
C67	FLA-24	$Fo_{15}Lc_{40}Ak_{45}$	780	3	Ks>Kf+Gl+V
C68	FLA-24	$Fo_{15}Lc_{40}Ak_{45}$	770	1	Ks>Kf>Ph+Gl+V

All assemblages contained an additional vapour phase. The symbols ≫, > etc indicate relative proportion of the phases. Abbreviations are same as those mentioned in the text.

[a] Run (C58) was re-run at 780 °C (C59) and 800 °C (C60) to see if the product is similar to run 57 and run 56, respectively. Runs reversed at lower temperature are indicated by letter (r).

anorthite (An) varying between 1 to 3.65 wt.% (Table 7). The maximum anorthite (An) content in the K-feldspar crystallized in the Fo–Di–Lc join is 1.4 wt.% and that in the join Fo–Lc–Ak is 1.75 wt.%. Kalsilite appears as hexagonal plates and could be identified from K-feldspar by its lower birefringence.

Merwinite appears only in the join Fo–Lc–Ak as prisms near the liquidus, and could be distinguished from diopside by its higher relief and lower birefringence. Electron microprobe analyses of merwinite shows that it contains 0.11–0.34 wt.% Al_2O_3 (Table 7).

3.2. The join forsterite–diopside–leucite at 0.1 GPa [P(H_2O) = P(Total)]

Gupta (1972) studied this join under atmospheric pressure (Fig. 2a). Forty-eight runs were made to study the join Fo–Di–Lc under 0.1 GPa [$P(H_2O) = P$(Total)] at variable temperatures to learn about the effect of H_2O on phase relationships in this join. These experimental results are summarized in Table 2 and Fig. 2b. The pseudo-eutectic point for the join Fo–Lc in presence of excess water has been estimated to be $Fo_{17}Lc_{83}$ ('B' in

Table 4
Electron microprobe analyses of glasses

Run no.	A46	A47	A48	B17	B24	B66	B67	B68	B69	B70
Mixture no.	FDL-27	FDL-27	FDL-27	FDL–4	FDL-5	FDL-22	FDL-22	FDL-22	FDL-22	FDL-23
Temp. (°C)	920	890	880	1150	1100	1230	1100	1020	1005	1010
Press. (GPa)	0.1	0.1	0.1	2.3	2.3	2.3	2.3	2.3	2.3	2.3
SiO_2	57.70	59.00	58.81	54.45	61.50	57.58	59.14	58.62	57.98	58.45
Al_2O_3	8.21	9.35	8.80	10.14	13.64	9.26	10.44	8.54	7.31	6.91
MgO	16.01	11.00	11.26	13.00	5.04	17.02	13.01	13.41	14.41	12.48
CaO	10.25	10.97	12.13	14.54	9.41	7.68	7.78	11.18	13.18	15.45
K_2O	7.68	8.76	8.03	6.29	9.05	8.38	9.64	7.93	6.41	6.21
Total	99.85	99.08	99.03	98.42	98.64	99.92	100.01	99.68	99.29	99.50

Run no.	B71	B72	C2	C21	C61	C64	C65	C66	C67	C68
Mixture no.	FDL-23	FDL-23	FLA-1	FLA-5	FLA-22	FLA-24	FLA-24	FLA-24	FLA-24	FLA-24
Temp. (°C)	1005	990	1240	1380	820	1265	1180	1165	780	770
Press. (GPa)	2.3	2.3	2.3	2.3	2.3	2.3	2.3	2.3	2.3	2.3
SiO_2	59.41	59.04	47.91	45.01	51.98	53.05	53.60	52.44	60.04	59.21
Al_2O_3	8.38	8.19	11.01	2.51	17.01	8.23	8.68	7.64	14.21	13.32
MgO	11.09	12.94	11.69	19.75	5.72	14.76	12.52	11.63	4.38	6.11
CaO	13.08	12.54	19.01	31.01	7.98	16.59	17.39	21.47	8.24	9.06
K_2O	7.66	7.54	9.21	1.98	15.86	7.58	8.00	7.00	13.00	12.33
Total	99.62	100.25	98.83	100.26	98.55	100.21	100.19	100.18	99.87	100.03

Table 5
Electron microprobe analyses of forsterite and diopside

Run no.	B5	C22	C35	B22	B27	B37	C5	C19	C20	C24
Phase	Fo	Fo	Fo	Di	Di	Di	Di	Di	Di	Di
Temp. (°C)	1005	1250	1300	950	975	805	1150	1200	1100	1230
Press. (GPa)	2.3	2.3	2.3	2.3	2.3	2.3	2.3	2.3	2.3	2.3
SiO_2	43.91	43.33	42.54	55.78	55.86	54.77	54.41	52.21	52.33	51.04
Al_2O_3	nd	nd	nd	3.57	1.35	6.18	4.90	4.11	4.04	5.05
MgO	56.34	57.14	55.67	19.42	18.86	18.01	18.60	18.41	18.99	16.15
CaO	0.19	0.22	0.15	20.09	23.23	18.86	21.16	26.01	24.22	25.68
K_2O	nd	nd	nd	0.29	0.24	1.07	0.39	0.01	0	0
Total	100.44	100.69	98.36	99.15	99.54	98.89	99.46	100.75	99.58	97.92
O=	4	4	4	6	6	6	6	6	6	6
Si	1.021	1.007	1.011	1.986	2.004	1.954	1.942	1.876	1.891	1.883
Al	nd	nd	nd	0.150	0.057	0.260	0.206	0.174	0.172	0.22
Mg	1.953	1.980	1.973	1.031	1.009	0.958	0.990	0.986	1.023	0.888
Ca	0.005	0.005	0.004	0.766	0.893	0.721	0.809	1.001	0.938	1.015
K	nd	nd	nd	0.013	0.011	0.049	0.018	0.000	0.000	0.000
Total	2.979	2.992	2.988	3.946	3.974	3.942	3.965	4.037	4.024	4.006

Fig. 2b) from Luth (1967), who studied the system Mg_2SiO_4–KA_lSiO_2–SiO_2–H_2O at 0.1 GPa [$P(H_2O)=P$(Total)]. The pseudo-eutectic point for the join Fo–Di was estimated to be at $Fo_{16.5}Di_{83.5}$ ('C'). From the study of the starting materials within the Fo–Di–Lc join, the pseudo-eutectic point ('D') for the Di–Lc join was determined in the present study, and was found to occur at $Di_{49.5}Lc_{50.5}$ at 885±5 °C. The five-phase point for the join Fo–Di–Lc occurs at 'A' ($Fo_3Di_{50}Lc_{47}$) and 880±5 °C, where forsteritess, diopsidess and leucitess are in equilibrium with liquid and vapour.

With reference to the study of the same join under 1 atmospheric pressure by Gupta (1972) (Fig. 2a), it is observed that in the presence of water the coexistence of $Fo_{ss}+Di_{ss}+Lc_{ss}+$Liq occurs at 880 °C which contrasts the presence of the same assemblage at 1296±5 °C (Fig. 2a) under one atmospheric pressure. The data show a drop of about 416 °C in the temperature of coexistence for these four phases. In presence of excess water the five-phase point ($Fo_{ss}+Di_{ss}+Lc_{ss}+$Liq+V) moves closer toward leucite, since such mafic phases as forsterite and diopside remains relatively insoluble compared to leucite. The shift in the composition of the five-phase point toward the feldspathoid end compared to the mafic end members, has also been observed by Yoder and Upton (1971). Another interesting feature of this study is the occurrence of phlogopite$_{ss}$ at 850 °C or below (runs A4, A5, A9, A16, A26 in Table 1). With reference to the study of Luth (1967) on the join Fo–Lc at 0.1 GPa [$P(H_2O)=P$(Total)], the presence of

Table 6
Electron microprobe analyses of phlogopite and leucite

Run no.	B26	B36	B37	C5	C59	C60	A8	A15	A22
Phase	Ph	Ph	Ph	Ph	Ph	Ph	Lc	Lc	Lc
Temp. (°C)	1005	850	805	1150	780	800	850	850	850
Press. (GPa)	2.3	2.3	2.3	2.3	2.3	2.3	0.1	0.1	0.1
SiO_2	42.13	43.44	48.85	42.45	37.71	38.92	54.41	54.98	55.15
Al_2O_3	17.48	16.18	16.34	19.51	21.38	18.53	23.29	23.20	23.23
MgO	23.43	27.19	22.05	25.42	24.13	25.75	0.06	0.05	0.08
K_2O	13.03	11.17	9.31	9.22	13.10	13.18	21.64	21.56	21.59
Total	96.07	97.98	96.55	96.60	96.32	96.38	99.40	99.79	100.05
O=	22	22	22	22	22	22	6	6	6
Si	5.851	5.858	6.498	5.724	5.266	5.440	1.992	2.002	2.002
Al	2.861	2.572	2.562	3.100	3.519	3.053	1.005	0.996	0.994
Mg	4.851	5.466	4.372	5.110	5.023	5.366	0.003	0.003	0.004
K	2.309	1.921	1.580	1.586	2.334	2.530	1.011	1.001	1.000
Total	15.872	15.817	15.012	15.520	16.142	16.389	4.011	4.002	4.000

Table 7
Electron microprobe analysis of K-feldspar, kalsilite, and merwinite

Run no.	B27	B36	B37	C58	C37	C38	C54	C37	C22	C35
Phase	Kf	Kf	Kf	Kf	Kf	Kf	Ks	Ks	Mer	Mer
Temp. (°C)	975	850	805	750	775	750	800	775	1250	1300
Press (GPa)	2.3	2.3	2.3	2.3	2.3	2.3	2.3	2.3	2.3	2.3
SiO_2	63.52	60.62	61.15	62.24	63.37	64.05	37.97	37.84	36.10	38.97
Al_2O_3	19.46	21.87	22.60	21.33	21.61	19.13	32.23	32.82	0.14	0.21
MgO	0.00	0.00	0.00	0.00	0.00	0.00	0.00	0.00	12.57	16.15
CaO	0.72	0.23	0.23	0.69	0.64	0.60	0.00	0.00	51.46	44.40
K_2O	14.81	13.49	14.00	14.23	14.17	15.96	29.77	29.67	0.00	0.00
Total	98.51	96.21	97.98	98.49	99.79	99.74	99.97	100.33	100.27	99.73
O=	8	8	8	8	8	8	4	4	8	8
Si	2.960	2.874	2.854	2.895	2.902	2.966	1.000	0.992	1.974	2.079
Al	1.069	1.222	1.243	1.169	1.167	1.044	1.000	1.014	0.009	0.013
Mg	0.00	0.00	0.00	0.00	0.00	0.00	0.00	0.00	1.025	1.284
Ca	0.036	0.012	0.011	0.034	0.031	0.030	0.000	0.000	3.014	2.538
K	0.880	0.816	0.833	0.844	0.828	0.943	1.000	0.992	0.000	0.000
Total	4.946	4.923	4.942	4.943	4.928	4.983	3.000	2.998	6.022	5.914

phlogopite along with forsterite and leucite agrees well with the present study.

On the basis of composition of the glasses in equilibrium with different phases (Table 4), the projected path of the liquid in this join is shown in Fig. 2b. The projected line of descent (a bold line with solid squares) is slightly off the phase boundary. Although a liquid and a vapour phase were found to coexist with crystalline phases in the quenching run products, the vapour phase together with the liquid probably existed in the form of a fluid phase during run. Because of the appearance of phlogopite and presence of vapour (or fluid), the join may be treated as a part of a quinary system, $KAlSiO_4$–CaO–MgO–SiO_2–H_2O.

3.3. The join forsterite–diopside–leucite studied under 2.3 GPa and variable temperatures

Seventy-two experimental runs (Table 2) were made to study this join under a condition of $P(H_2O)=P(Total)$ at variable temperatures. The results are summarized in Fig. 3a, which shows that the join penetrates the phase volumes of forsterite$_{ss}$, phlogopite$_{ss}$, diopside$_{ss}$, K-feldspar$_{ss}$ and kalsilite. There are three five-phase points: 1) 'B' ($Fo_9Di_{49}Lc_{42}$ and 1005±10 °C), where forsterite$_{ss}$, diopside$_{ss}$ and phlogopite$_{ss}$ coexist with liquid and vapour, 2) 'C' ($Fo_4Di_{50}Lc_{46}$ and 990±10 °C), where phlogopitess, diopsidess and K-feldsparss are in equilibrium with liquid and vapour, and 3) 'D' ($Fo_3Di_{21}Lc_{76}$ and 775±5 °C), where phlogopitess, kalsilite and K-feldspar$_{ss}$ are in equilibrium with liquid and vapour. The presence of K-feldspar$_{ss}$ and kalsilite are related to breakdown of leucite under high P–T conditions (Fashauer et al., 1998; reaction (1)). Formation of phlogopitess in this join is related to the reaction involving forsterite, leucite and vapour to produce phlogopite$_{ss}$ and K-feldspar$_{ss}$ (reaction (2)) (Yoder, 1986).

In case of the Fo–Di–Lc join studied at one atmosphere, the piercing point 'I' ($Fo_{ss}+Di_{ss}+Lc_{ss}+Liq$) occurs at $Fo_2Di_{67}Lc_{31}$ and 1296 °C (Gupta, 1972) (Fig. 2a). However, in the present study conducted at 2.3 GPa [$P(H_2O)=P(Total)$] (Fig. 3b), all the three five-phase points occurring at 'B' (1005 °C), 'C' (990 °C) and 'D' (775 °C) have liquidus temperatures significantly lower than that of piercing pint 'I' (Fig. 2a), because the present investigation has been conducted in the presence of excess water [$P(H_2O)=P(Total)$]. Compared to the phase equilibrium study conducted at one atmospheric pressure (Fig. 2a) and 0.1 GPa (Fig. 2b), the study of the same join at 2.3 GPa shows significant difference (Fig. 3a). At 2.3 GPa phlogopite$_{ss}$, kalsilite, and K-feldspar$_{ss}$ are additional phases and leucite is completely absent. Microprobe analyses of glasses in the join Fo–Di–Lc at 2.3 GPa [$P(H_2O)=P(Total)$] and variable temperatures (Table 4) is projected on to this join from the H_2O apex (bold line with solid squares) (Fig. 3b). Although projected paths of the melts are slightly off the phase boundaries, nevertheless the crystallization trends are consistent with the observed sequence of crystallization, as given in Table 2.

3.4. The join forsterite–leucite–åkermanite studied at 2.3 GPa and variable temperatures

The phase relations in the join Fo–Lc–Ak were studied at 1 atmospheric pressure by Gupta (1972) (Fig. 4a). In this study, sixty-eight runs were made to investigate the join Fo–Lc–Ak at 2.3 GPa [$P(H_2O)=$

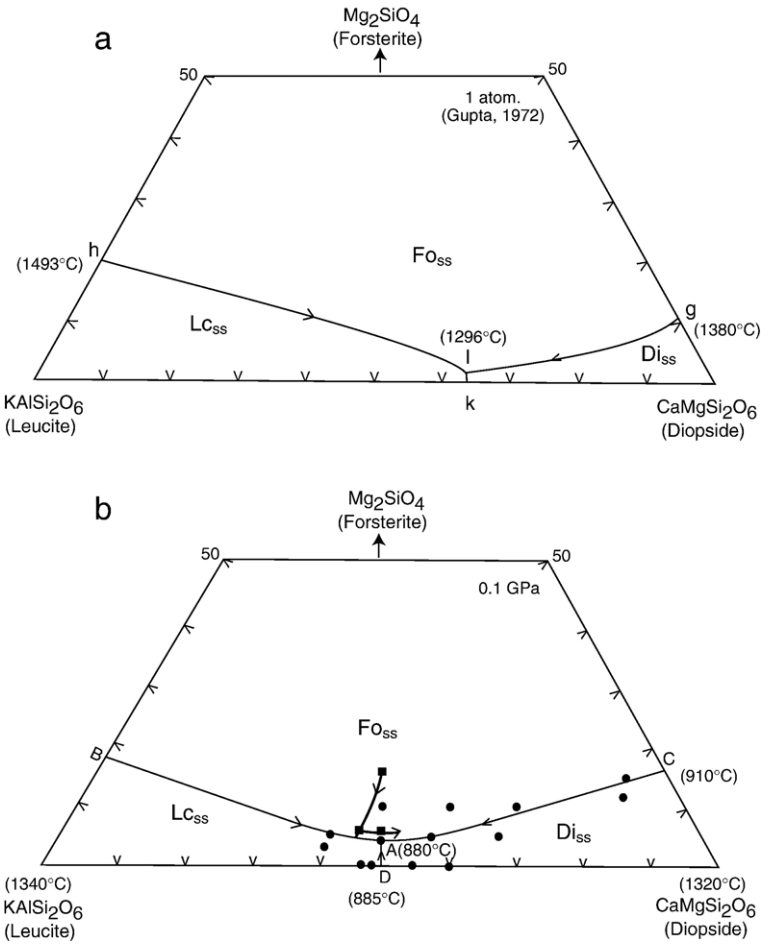


Fig. 2. (a). Phase relations in the join Fo–Di–Lc studied under atmospheric pressure (after Gupta, 1972). (b) Phase relations in the join Fo–Di–Lc studied under 0.1 GPa [$P(H_2O)=P(Total)$] (present study). The bold line with squares is a projected path of the liquid as determined from the composition of glasses in equilibrium with crystalline phases.

P(Total)]. The results are summarized in Table 3 and Fig. 4b, which show that the join intersects the primary phase volumes of forsterite$_{ss}$, phlogopite$_{ss}$, kalsilite, K-feldspar$_{ss}$, diopside$_{ss}$ and merwinite$_{ss}$. There are 4 five-phase points occurring at following compositions and temperatures: 1) 'N' ($Fo_7Lc_{42}Ak_{51}$ and 1165± 10 °C), where phlogopite$_{ss}$, forsterite$_{ss}$ and diopside$_{ss}$ coexists with liquid and vapour, 2) 'O' ($Fo_3Lc_{49}Ak_{48}$ and 1140±10 °C), where a liquid is in equilibrium with phlogopitess, K-feldsparss, diopsidess and vapour, 3) 'M' ($Fo_{13}Lc_{21}Ak_{66}$ and 1255±10 °C), where merwinite$_{ss}$, forsterite$_{ss}$ and diopside$_{ss}$ are in equilibrium with liquid and vapour, and 4) 'P' ($Fo_{5.5}Lc_{73.5}Ak_{21}$, and 775± 10 °C), where kalsilite, phlogopite$_{ss}$ and K-feldspar$_{ss}$ coexist with liquid and vapour (Fig. 4b).

When the phase relationships in the join Fo–Lc–Ak at one atmospheric pressure (Gupta, 1972) (Fig. 4a) is compared with those at 2.3 GPa (Fig. 4b), it may be noted that there is a field of monticellite$_{ss}$ occurring near the join Fo–Ak. In contrast, Fig. 5b shows the presence of a field of merwinitess as suggested by Yoder (1973). The piercing point 'G' ($Fo_{ss}+Ak_{ss}+Lc_{ss}+Liq$) observed in this join at one atmospheric pressure (Gupta, 1972) occurs at 1286 °C, whereas the temperatures of the five-phase points 'N' (1165 °C), 'O' (1140 °C), 'M' (1255 °C) and 'P' (770 °C) are significantly lower, because the present study at 2.3 GPa was conducted under a condition of $P(H_2O)=P$(Total). The comparison of the two figures (Fig. 5a and b) shows that in case of the 2.3 GPa isobaric diagram there are such additional phases as phlogopite$_{ss}$, K-feldspar$_{ss}$, kalsilite and merwinite$_{ss}$, which are absent in the one atmospheric phase diagram of the same join (Fig. 4a). Microprobe analyses of glasses at 2.3 GPa [$P(H_2O)=P$(Total)] and variable temperatures (Table 4) are shown in Fig. 4c, where the trends of liquid composition (bold

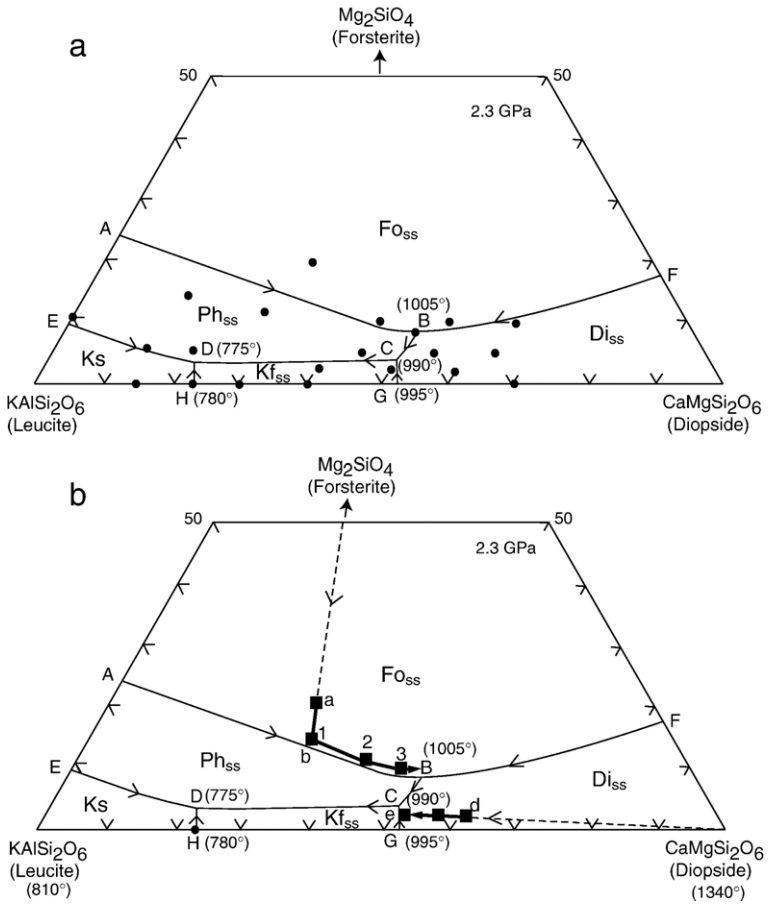


Fig. 3. (a). Phase relations in the join Fo–Di–Lc studied under 2.3 GPa [$P(H_2O)=P(\text{Total})$] (present study). (b) Course of crystallization of liquid in the join Fo–Di–Lc studied under 2.3 GPa [$P(H_2O)=P(\text{Total})$] (present study). The bold line with squares is a projected path of the liquid as determined from the composition of glasses in equilibrium with crystalline phases.

lines with solid squares) are projected on to the Fo–Lc–Ak join from the H_2O apex. Although the trends of liquid compositions do not coincide with the exact phase boundaries, the course of crystallization is consistent with the observed sequence of crystallization (Table 3).

3.5. The paragenetic sequence in the kalsilite–CaO–MgO–SiO_2–H_2O system

If a small amount of alumina present in diopside as $CaAl_2SiO_6$ molecule is ignored, the system may then be treated as quinary having the following components, kalsilite–CaO–MgO–SiO_2–H_2O. It is further assumed that the vapour phase observed in the glasses should combine under elevated P–T condition as a fluid phase (f) and the remaining water is dissolved in the crystalline phases. Because of this and presence of some components as solid solution in different phases, the system in effect behaves as a four-component system. On these assumptions, a flow-sheet diagram is drawn, as shown in Fig. 5. This helps us to draw the paragenetic sequence in the four-component system near the points B and C (Fig. 3) and also near the points 'N' and 'O' (Fig. 4). At the invariant point 'X' (975 ± 10 °C, Fig. 5), the number of phases is five ($Fo_{ss}+Di_{ss}+Ph_{ss}+Kf_{ss}+f$) as expected for a four-component system (see runs B11, B16 and B27 in Table 2). Following the Scheinemaker's rule there should be four univariant lines leading to the five-phase invariant point 'X'. The four univariant lines 361 should be Fo_{ss}–Di_{ss}–Ph_{ss}–f, Kf_{ss}–Di_{ss}–Fo_{ss}–f, Kf_{ss}–Ph_{ss}–Fo_{ss}–f, and Ph_{ss}–Kf_{ss}–Di_{ss}–f.

Likewise, the five-phase invariant assemblage near the point 'D' (Fig. 3) comprises Ph_{ss}, Ks, Kf_{ss}, Di_{ss} and f, requires that there should be four univariant lines namely: 1) Kf_{ss}–Ph_{ss}–Ks–f, 2) Ph_{ss}–Kf_{ss}–Di_{ss}–f, 3) Kf_{ss}–Di_{ss}–Ks–f, and 4) Ks–Ph_{ss}–Di_{ss}–f. It is noted that the five-phase invariant assemblage (Ks–Ph_{ss}–Kf_{ss}–

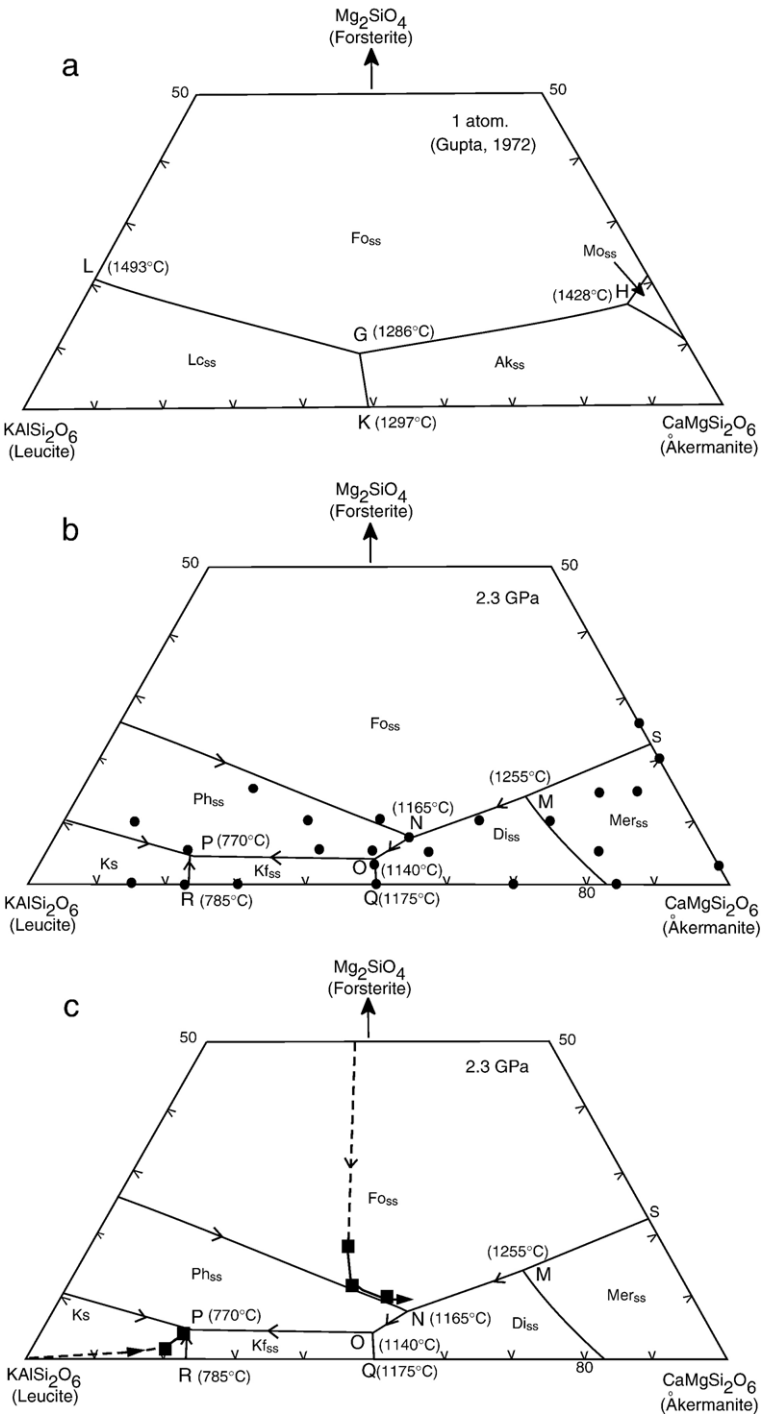


Fig. 4. (a) Phase relations in the join Fo–Lc–Ak at one atmospheric pressure (after Gupta, 1972). (b) Phase relations in the join Fo–Lc–Ak at 2.3 GPa [$P(H_2O)=P(Total)$] (present study). (c) Course of crystallization of melts in the join Fo–Lc–Ak at 2.3 GPa [$P(H_2O)=P(Total)$] (present study). The bold line with squares is a projected path of the liquid as determined from the composition of glasses in equilibrium with crystalline phases.

Pi_{ss}–f) is obtained at 775±10 °C (see runs B56, B57 in Table 2). Since the four-phase univariant assemblage (Ph_{ss}–Kf_{ss}–Di_{ss}–f) is common to both the invariant points 'X' and 'Y' (Fig. 5), there has to be a thermal barrier originating from the point "O" (1140±10 °C). This univariant assemblage, Ph_{ss}–Fo_{ss}–Di_{ss}–f also

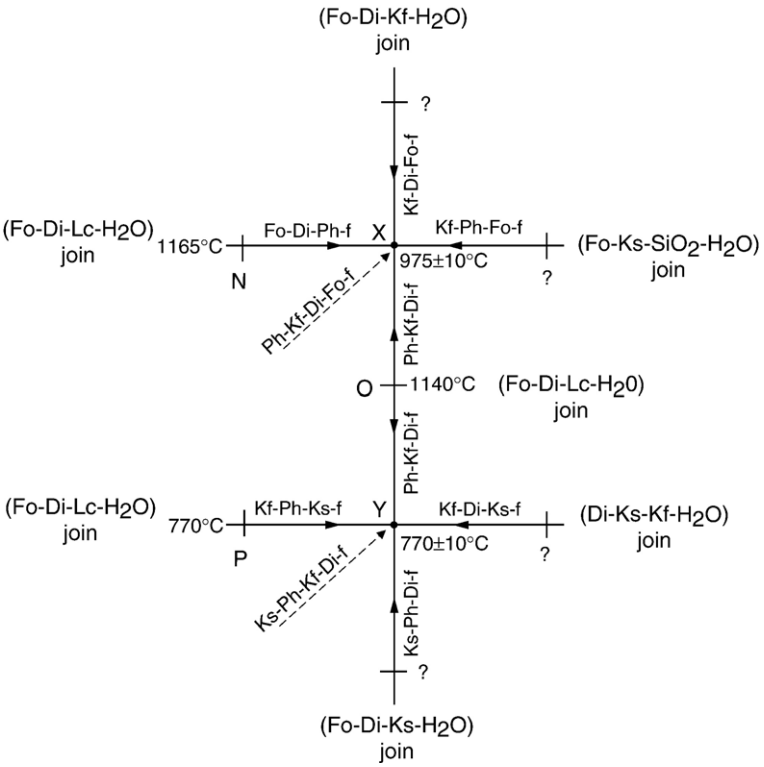


Fig. 5. The flow-sheet diagram showing paragenetic relationships of various assemblages in the join Fo–Di–Lc–H_2O studied under 2.3 GPa and variable temperatures. In drawing the flow-sheet diagram it has been assumed that liquid + vapour observed in the products were present as fluid under elevated *P–T* conditions. It should be pointed out that the flow sheet diagram for the join forsterite–leucite–åkermanite–H_2O should be similar to this diagram. There is some difference in that the univariant line (Fo + Di + Ph + f) in the Fo–Lc–Ak–H_2O join is derived from the univariant line (Fo + Mer + Di + f). As merwinite reacts with the liquid and is eliminated, the melt composition follows a divariant surface (Fo + Di + f) and then moves along the univariant line (Fo + Ph + Di + f) and finally moves towards the point 'X' (Ph + Kf + Di + Fo + f).

originates at point 'N' (1165 ± 10 °C). Likewise, the univariant assemblage (Kf_{ss}–Ph_{ss}–Ks–f) originates at the point "P" (765 ± 10 °C) (Fig. 4).

The paragenetic sequence of different simplified rock types in the join Fo–Lc–Ak is similar to the flow sheet diagram as shown in (Fig. 5). There is some difference, however, in that the univariant line (Fo_{ss}–Di_{ss}–Ph_{ss}–f) in the join Fo–Lc–Ak–H_2O, is derived from the assemblage (Fo_{ss}–Mer_{ss}–Di_{ss}–f). As merwinite$_{ss}$ reacts with the liquid and is eliminated, the melt composition follows a divariant surface (Fo_{ss}–Di_{ss}–Ph_{ss}–f) and finally to the point (Fo_{ss}–Di_{ss}–Ph_{ss}–Kf_{ss}–f) (Fig. 5).

4. Petrological significance

4.1. The join forsterite–diopside–leucite studied under 0.1 GPa [P(H_2O) = P(Total)]

With reference to Fig. 2b, it should be stated that the five-phase point A corresponds to an olivine leucitite termed as ugandite by Holmes (1942). Fig. 2b further suggests that ugandite can be derived from an olivine italite (along B–A), a leucitite (along D–A), and a K-rich olivine–pyroxene rich magma (along C–A). With lowering of temperature, phlogopite$_{ss}$ precipitates along with olivine, leucite$_{ss}$, and pyroxene$_{ss}$ at 850 ± 10 °C (Table 1). This phlogopite-bearing assemblage corresponds to a rock called missourite or kajanite [equivalent to mica-rich ugandite by Lacroix, 1926]. Holmes (1942, 1950) recognized that ugandite is one of the most primitive magmas in the Western branch of the African Rift. Cross (1897) coined the term wyomingites to a rock composed of leucite, olivine, augite and phlogopite (also see Yagi and Matsumoto, 1966; Carmichael, 1967). The assemblage (Ph_{ss} + Fo_{ss} + Lc_{ss} + Di_{ss} + Liq) at 850 ± 10 °C (Table 1) is comparable to woymingite. Barton and Hamilton (1979, their Fig. 1) studied melting phase relationships of a natural madupite composition below 0.4 GPa. At temperatures below 1150 °C, they obtained the assemblage (Cpx + Ph + Ol + Lc + Liq). This assemblage is similar to that obtained near point 'A' around 800 ± 10 °C (Table 1).

In various localities of New South Wales such as Lake Cargello, Begargo Hills, Flag Staff Hills, Bygoloric, and Condobline, there are olivine leucitites containing phlogopite. Such rocks called missourite are also reported from Gaussberg, Antarctica (Sheraton and Cundari, 1980) and from Mount Jugo and Colli–Albani Volcanic fields of Italy (Cundari, 1973). They however, described these rocks simply as leucitite without taking into consideration the presence of olivine and phlogopite.

4.2. The join forsterite–diopside–leucite studied under 2.3 GPa at variable temperatures

With reference to Fig. 3b and Table 2, from a liquid of composition 'a' ($Fo_{20}Di_{30}Lc_{50}$) forsterite$_{ss}$ crystallizes first at 'b' (melt composition '1', Fig. 3b), phlogopite$_{ss}$ starts to precipitate in addition to forsterite$_{ss}$. The composition of liquid then moves along a multi-saturation line 'b-B' to 'B' (near melt composition '3'), where diopside$_{ss}$ co-precipitates with forsterite$_{ss}$ and phlogopite$_{ss}$. With the lowering of temperature further, K-feldspar$_{ss}$ appears at 985±10 °C (Table 2). Thus the final assemblage comprises forsterite$_{ss}$ + phlogopite$_{ss}$ + diopside$_{ss}$ + K-feldspar$_{ss}$ and liquid. The assemblage along 'b-B' corresponds to a madupite, a type locality of which is Pilot Butte at Leucite Hills. The assemblage forsterite + phlogopite + clinopyroxene corresponds to missourite or kazanite. The final crystalline product comprising phlogopite$_{ss}$, diopside$_{ss}$, forsterite$_{ss}$, and K-feldspar$_{ss}$ similar to a phenocryst assemblage of olivine–pyroxene minette.

Makhotkin et al. (1989) described lamproites comprising olivine, phlogopite and diopside from Khani (57°54′ N, 120°46′ E) and Ryabinovaya (57°40′ N, 125°51′ E) of Aldan alkaline province of Russia. This assemblage corresponds to that of the five-phase point 'B' (Fig. 3b). The lamproite of Rayabinovaya is associated with a phlogopite-bearing minette. There is also brecciated pipe (600–700 m long) at Kaila of the same petrographic province of Aldan. The pipe is constituted of olivine, diopside, and phlogopite phenocrysts with clinopyroxene, phlogopite, and K-feldspar occurring in the groundmass, as is the near solidus assemblage (point 'X' in Fig. 4). Similarly, O'Brien et al. (1991) described olivine minettes from Highwood Mountains, Montana, U.S.A., which have the seriate porphyritic texture with phenocrysts of phlogopite, clinopyroxene and forsteritic olivine (Fo87–92) in a matrix of sanidine, clinopyroxene, phlogopite and glass.

From a liquid of composition 'd' ($Fo_3Di_{60}Lc_{37}$) (Fig. 3b), diopsidess precipitates first at 1010 °C, followed by K-feldsparss as the second phase at 'e', then phlogopite appears at 990 °C (at point 'C') as the third phase (see crystallization sequence for the 436 composition $Fo_3D_{60}Lc_{37}$ in Table 2). The assemblage diopsidess + liquid corresponds to diopsidite, whereas the assemblage along 'e-C' (Di_{ss} + Kf_{ss} + Liq) corresponds to pyroxene-bearing syenite, and the assemblage at 'C' (Di_{ss} + Kf_{ss} + Ph_{ss} + Liq) corresponds to pyroxene-bearing minette. With further lowering of temperature, the final assemblage comprises diopside$_{ss}$, K-feldspar$_{ss}$, phlogopite$_{ss}$, kalsilite$_{ss}$, and liquid (Table 2). This assemblage corresponds to kalsilite–pyroxene minette. If a kalsilite–pyroxene minette magma ascends upward quickly, leucite should appear at shallower depth before K-feldspar$_{ss}$ and kalsilite$_{ss}$ completely disappear (Fig. 3a). Bhowmik (2000) described diopsidite veinlets in association with rocks comprising K-feldspar, kalsilite, phlogopite, leucite, and diopsidic pyroxene from the ductile shear zones of Borra near Visakapatnam, south India. Such kalsilite–K-feldspar-bearing rocks have also been reported from the Punalur locality of southern India (Sandiford and Santosh, 1991). This assemblage is comparable to the end product crystallizing from a liquid composition 'D' in the Fo–Di–Lc–H_2O join (Fig. 3b).

MacDonald et al. (1992) described minettes from Bearpaw Mountains, which are characterized by the presence of olivine and clinopyroxene phenocrysts in a groundmass of phlogopite and sanidine. This assemblage is comparable to the five-phase point 'C' (Ph_{ss} + Kf_{ss} + Di_{ss} + Liq + V) (Fig. 3) and corresponds to pyroxene-bearing minette. As the composition closed to 'C' contains only 3% forsterite, olivine is consumed in the formation of phlogopite and K-feldspar. See the reaction below:

$$3Fo + 3Lc = 2Ph + Kf \quad (6)$$

The assemblage at point 'D' (Fig. 3) is characterized by the assemblage kalsilite$_{ss}$, K-feldspar$_{ss}$, phlogopite$_{ss}$ and liquid. This assemblage is equivalent to kalsilite-bearing minette. Orlova et al. (1986) described phlogopite-bearing yakutite (phlogopite + K-feldspar + clinopyroxene + kalsilite) from Malomurunskii ultrapotassic complex. This assemblage is noted in a stratified lopolith. This complex has a lower layer comprising phlogopite and pyroxene at the bottom followed upward by a layer with the assemblage consisting of kalsilite, K-feldspar and clinopyroxene. We believe that a kalsilite-bearing minette magma, having an assemblage similar to the five-phase point 'C' cooled slowly and the phlogopite and pyroxene-rich fraction settled at the bottom leaving behind a kalsilite–clinopyroxene–K-feldspar-bearing residue (kalsilite syenite) observed in that locality.

Gupta and Green (1988) studied the system kalsilite–forsterite–silica at 2.8 GPa [$P(H_2O)=P(Total)$]. They also observed the presence of a five-phase assemblage of $Ph_{ss}+Ks+San_{ss}+L+V$ similar to Figs. 3b and 5b. Foley et al. (1986) added 4 wt.% F to see the effect of F on the topology of Fo–Ks–SiO_2 phase diagram. They observed that their phase diagram broadly resembled the water-saturated F-free system of Gupta and Green (1988) in having a large primary phase volume for phlogopite plus primary phase volumes as such minerals as forsterite, kalsilite and sanidine. Foley et al. (1986) found that F-bearing system differs in that the fluorphlogopite has a much greater thermal stability (maximum 1490–1500 °C) than hydroxyphlogopite (<1200 °C: Gupta and Green, 1988).

4.3. The join forsterite–leucite–åkermanite studied at 2.3 GPa and variable temperatures

Phase relations in the leucite-rich section of the join Fo–Lc–Ak (Fig. 5b) is very similar to those of the join Fo–Di–Lc studied at 2.3 GPa (Fig. 3a) in that there are primary phase fields of $forsterite_{ss}$, $phlogopite_{ss}$, $K\text{-}feldspar_{ss}$, $kalsilite_{ss}$ and $diopside_{ss}$ in the åkermanite-poor region of the join (Fig. 4b). Comparing Figs. 3a and 4b, it may be stated that the paragenetic relationship in the leucite-rich but åkermanite-poor (<60 wt.% åkermanite) section of the join is very similar to that already described in the previous section. With reference to Fig. 4b, it may be observed that the assemblage at 'N' ($Fo_7Lc_{40}Ak_{53}$; 1165±10 °C) corresponds to olivine-bearing madupite. Like phase relations in Fig. 3a, with the lowering of temperature at point 'N', the final assemblage near the solidus is constituted of forsteritess, phlogopitess, diopsidess, $K\text{-}feldspar_{ss}$, liquid, and vapour. This assemblage corresponds to olivine–pyroxene-bearing minette. Lloyd et al. (1985) investigated melting phase relationships of an olivine melilite glass under variable P–T conditions and noted the above mentioned reaction (7). The assemblage obtained by them from the olivine melilite glass is similar to that obtained near the solidus close to point 'N' (Fig. 4b). If such a liquid coexisting with forsterite, phlogopite, clinopyroxene and K-feldspar ascends near the surface, it would result in an assemblage comprising $forsterite_{ss}+åkermanite_{ss}+leucite_{ss}+$liquid (katungite).

The join Fo–Lc–Ak was studied by Gupta (1972) at one atmosphere (Fig. 4a) and he showed that katungite magma (olivine+melilite+leucite+liquid) can be obtained from the following parental liquids: monticellite alnoite ('H' in Fig. 4a), melilite italite ('K', Fig. 4a) or olivine italite ('L', Fig. 4a). With reference to the study of the same join at 2.3 GPa, it may be observed that kalsilite-bearing minette, pyroxene-bearing minette and olivine–pyroxene-bearing minette have heteromorphic high pressure equivalents of katungite. Likewise, monticellite alnoite (Fig. 4a, åkermanite-rich side) is represented at high pressure by merwinite-bearing websterite.

Appearance of merwinitess and diopsidess is related to the breakdown of åkermanite (Yoder, 1973) because of the reaction (4) described earlier. Yoder (1973) showed that below 0.62 GPa and 750 °C åkermanite breaks down to monticellite+wollastonite. Yoder noted that formation of a merwinite and diopside at the expense of åkermanite and forsterite is valid up to 1.05 GPa and 1090 °C, and above this pressure diopside and merwinite should be the stable products at the expense of forsterite and åkermanite.

Arima and Edgar (1983a) studied melting relationships of the katungite composition at pressures up to 3.5 GPa and temperatures to 1300 °C. They observed that below 2 GPa in the presence of excess water olivine appeared as the liquidus phase, but it disappeared at lower temperatures because of reaction with liquid. Their data indicate that clinopyroxene together with phlogopite has a wide P–T range of stability. Melilite appeared only below 1.0 GPa. At high pressure (2.3 GPa) but low temperatures toward the leucite-rich side, instead of a breakdown product of åkermanite to form merwinite and diopside, åkermanite reacts with forsterite, leucite and vapour to produce phlogopite and diopside. Note the reaction:

$$5Fo + 3Lc + Ak + 3H_2O = 3Ph + 2Di \quad (7)$$

Thus, at 2.3 GPa and low temperatures towards the leucite-rich side above reactions inhibits the presence of $merwinite_{ss}$, which disappears and $diopside_{ss}$ together with $phlogopite_{ss}$ precipitates as suggested by the above reaction. Merwinite has not been reported in the K-rich mafic rocks, as it is eliminated at low temperatures because of the above reaction. Near the surface, equilibrium crystallization of a liquid lying in the Fo–Lc–Ak join has been described by Gupta (1972). He showed that a katungite magma (point 'G' in Fig. 4a), where liquid coexists with $forsterite_{ss}+leucite_{ss}+$åkermanite can be derived from monticellite alnoite, melilite italite or olivine italite. The assemblage at 2.3 GPa shows that katungite has heteromorphic reaction to olivine-bearing madupite ('N'), minette ('O') or kalsilite minette ('P') (Fig. 4b). At low pressure, the final assemblage might correspond to katungite. The univariant equilibrium involving reaction (2) (Ph=3Fo+Lc+Ks+V) has been identified by Holmes (1942), who described lava flows

containing clinopyroxene, kalsilite, olivine, melilite and leucite from the western limb of the African rift valley system (also see Yoder, 1986).

In summary, our experimental data demonstrate that high-pressure crystal differentiation can produce various types of K-rich mafic and ultramafic igneous rocks. The data suggest that olivine leucitite (ugandite) can be derived from olivine italite. The paragenetic relationships is inferred for phlogopite-bearing madupite, pyroxene-bearing minette, and kalsilite-bearing minette. The data further suggests that katungite has heteromorphic reaction to olivine-bearing madupite, pyroxene-bearing minette, and kalsilite-bearing minette. The phlogopite-bearing clinopyroxenite xenoliths commonly found in kamafugitic rocks (cf. Lloyd and Bailey, 1975; Lloyd et al., 2002) would probably represent high-pressure crystallization products derived from kamafugitic magmas.

Acknowledgements

The manuscript was greatly improved by the thoughtful and constructive reviews of R.V. Conceicaoção and an anonymous reviewer. A.K. Gupta thanks the Department of Science and Technology (India) for providing funds (No. IR/S-4/ESF-01/03) to complete this work. K. Nag thanks the authorities of the Oil and Natural Gas Corporation for allowing him to publish this manuscript.

References

Arima, M., Edgar, A.D., 1983a. High pressure experimental studies on a katungite and their bearing on the genesis of some potassium-rich magmas of the west branch of the Africa-rift. Journal of Petrology 24 (2), 166–187.

Arima, M., Edgar, A.D., 1983b. A high pressure experimental study on a magnesian-rich leucite–lamproite from the West Kimberley area, Australia: petrogenetic implications. Contributions to Mineralogy and Petrology 84, 228–234.

Barton, M., Hamilton, D.L., 1979. The melting relationship of a madupite from Leucite Hills Wyoming, to 30 kbar. Contributions to Mineralogy and Petrology 66, 41–49.

Bhowmik, S.K., 2000. Ultrapotassic rocks along late ductile shear zones from the Eastern Ghats Belt India. Gondwana Research 3 (1), 55–63.

Bohlen, S.R., Essene, E.J., Boettcher, A.L., 1980. Reinvestigation and application of olivine–quartz–orthopyroxene-boundary. Earth and Planetary Science Letters 47, 1–10.

Bose, K., Ganguly, J., 1995. Quartz–coesite transition revised: reversed experimental determination at 500–1200 °C and retrieved thermochemical data. American Mineralogist 80, 231–239.

Boyd, F.R., England, J.L., 1960. Apparatus for phase-equilibria measurements at pressures up to 50 kilobars and temperatures up to 1759 °C. Journal of Geophysical Research 65, 741–748.

Carmichael, I.S.E., 1967. The mineralogy and petrology of the volcanic rocks from the Leucite Hills Wyoming. Contributions to Mineralogy and Petrology 15, 24–66.

Cross, W., 1897. The Igneous rocks of the Leucite Hills and Pilot Butte Wyoming. American Journal of Science 4, 115–141.

Conceicaoção, R.V., Green, D.H., 2000. Behavior of the cotectic curve En–Ol in the system leucite–olivine–quartz under dry conditions to 2.0 GPa. Geochemistry, Geophysics, Geosystems 1 (200GC000071).

Conceicaoção, R.V., Green, D.H., 2004. Derivation of potassic (shoshonitic) magmas by decompression melting of phlogopite+pargasite lherzolite. Lithos 72, 209–229.

Cundari, A., 1973. Petrology of the leucite-bearing lavas in New South Wales. Journal of the Geological Society of Australia 20, 465–492.

Fasshauer, D.W., Wunder, B., Chatterjee, N.D., Hohne, G.W.H., 1998. Heat capacity of wadeite-type $K_2Si_4O_9$ and the pressure-induced stable decomposition of K-feldspar. Contributions to Mineralogy and Petrology 131, 210–218.

Foley, S.F., 1992. Petrological characterization of the source components of potassic magmas: geochemical an experimental constraints. Lithos 28, 187–204.

Foley, S.F., Taylor, W.R., Green, D.H., 1986. The role of fluorine and oxygen fugacity in the genesis of the ultrapotassic rocks. Contributions to Mineralogy and Petrology 94, 183–192.

Foley, S.F., Venturelli, G., Green, D.H., Toscani, L., 1987. The ultrapotassic rocks: characteristics, classification, and constraints for petrogenetic models. Earth-Science Reviews 24, 81–134.

Gupta, A.K., 1972. The system forsterite–diopside–akermanite–leucite and its significance in the origin of potassium-rich mafic and ultramafic rocks. American Mineralogist 57, 1242–1259.

Gupta, A.K., Green, D.H., 1988. Experimental study of the system forsterite–kalsilite–SiO_2 in presence or absence of volatiles (CO_2) or H_2O) under 28 kb. Mineralogy and Petrology 39, 163–174.

Gupta, A.K., Yagi, K., 1980. Petrology and Genesis of Leucite-Bearing Rocks. Springer-Verlag, Berlin. 252 pp.

Gupta, A.K., Chattopadhyay, B., Fyfe, W.S., Powell, M., 2002. Experimental studies on three potassium-rich ultramafic rocks from Damodar Valley East India. Mineralogy and Petrology 74, 343–360.

Holmes, A., 1942. A suit of volcanic rocks from southwest Uganda containing kalsilite (a polymorph of $KAlSiO_4$). Mineralogical Magazine 26, 167–217.

Holmes, A., 1950. Petrogenesis of katungite and its associates. American Mineralogist 35, 772–792.

Lacroix, A., 1926. La systematique des roches leucitiques; les types de la famille syentique. Academic Science Comptes Rendu 182, 597–601.

Lloyd, F.E., Bailey, D.K., 1975. Light element metasomatism of the continental mantle: the evidence and consequence. Physics and Chemistry of the Earth 9, 389–416.

Lloyd, F.E., Arima, M., Edgar, A.D., 1985. Partial melting of a phlogopite linopyroxenite from south-west Uganda: an experimental study bearing on the origin of highly potassic continental rift volcanism. Contributions to Mineralogy and Petrology 91, 321–329.

Lloyd, F.E., Woolley, A.R., Stoppa, F., Eby, G.N., 2002. Phlogopite–biotite parageneses from the K-mafic-carbonatite effusive magmatic association on Katwe–Kikorongo SW Uganda. Mineralogy and Petrology 74, 299–322.

Luth, W.C., 1967. Studies in the system $KAlSiO_4$–Mg_2SiO_4–SiO_2–H_2O: I. Inferred phase relations and applications. Journal of Petrology 8, 372–416.

MacDonald, R., Upton, B.G., Collerson, K.D., Hearn, B.C., James, D., 1992. Potassic lavas of the Bearpaw Mountains, Montana: mineralogy, chemistry and origin. Journal of Petrology 33 (2), 305–346.

Makhotkin, I.I., Arakelyanz, M.M., Vladykin, N.V., 1989. On the age of the lamproites of the Aldan Province Doklad. Doklady Akademii Nauk SSSR 306, 703–707.

Melzer, S., Foley, S., 1996. Phase relationships of phlogopite in the system $KAlSiO_4$–Mg_2SiO_4–SiO_2–F and the stability of F-phlogopite at atmospheric pressure, 10 and 18 kbar. Neues Jahrbuch fur Mineralogie. Abhandlungen 171, 1–31.

Mitchell, R.H., Bergman, S.O., 1991. Petrology of Lamproites. Plenum, New York, p. 441.

Modreski, P., Boettcher, A.L., 1973. Phase relationships of phlogopite in the system K_2O–MgO–CaO–Al_2O_3–SiO_2–H_2O to 35 kilobars: a better model for micas in the interior of the Earth. American Journal of Science 273, 358–414.

O'Brien, H.E., Irving, A.J., McCallum, I.S., 1991. Eocene potassic magmatism in the Highwood Mountains, Montana; petrology, geochemistry and tectonic implications. Journal of Geophysical Research 96, 13237–13260.

Orlova, M.P., Ardontsev, S.N., Shchadenkov, E.M., 1986. Alkaline magmatism of the Aldan shield and its specific mineralogical features. In: Frunmkin, I.M. (Ed.), Geology and Geochemistry of the Ore-Bearing Magmatic and Metasomatic Associations from the Maly BAM Area Yakutia Branch of the Siberian Division of the USSR. Academy of Sciences, Yakutsk, pp. 4–12.

Rock, N.M.R., 1991. Lamprophyres. Blackie, Glasgow, p. 285.

Sandiford, M., Santosh, M., 1991. A granulite facies kalsilite–leucite–hibonite association from Punalur Southern India. Mineralogy and Petrology 43, 225–236.

Scarf, C.M., Luth, W.C., Tuttle, O.F., 1966. An experimental study bearing on the absence of leucite in plutonic rocks. American Mineralogist 51, 726–735.

Schairer, J.F., 1950. The alkali feldspar join in the system NaAlSiO4–$KAlSiO_4$–SiO_2. Journal of Geology 58, 512–517.

Schairer, J.F., Bowen, N.L., 1938. The system leucite–diopside–silica. American Journal of Science 35A, 289–309.

Sheraton, J.W., Cundari, A., 1980. Leucites from Gaussberg, Antarctica. Contributions to Mineralogy and Petrology 71, 417–427.

Veksler, I.V., Fedorchuk, Y.M., Nielsen, T.F.D., 1998. Phase equilibria in the silica-undersaturated part of the $KAlSiO_4$–Mg_2SiO_4–Ca_2SiO_4–SiO_2–F system at 1 atom and the larnite-normative trend of melt evolution. Contributions to Mineralogy and Petrology 131, 347–363.

Warner, R.D., Luth, W.C., 1973. Two phase data for the join monticellite ($CaMgSiO_4$)–forsterite ($MgSiO_4$): experimental study and numerical analyses. American Mineralogist 58, 998–1008.

Wendlandt, R.F., 1984. An experimental and theoretical analysis of partial melting in the system $KAlSiO_4$–CaO–MgO–SiO_2–CO_2 and applications to the genesis of potassic magmas, carbonatites and kimberlites. In: Kornprobst, J. (Ed.), Kimberlites and Related Rocks. Elsevier, Amsterdam, pp. 359–369.

Wendlandt, R.F., Eggler, D.H., 1980a. The origins of potassic magmas: 1. Melting relations in the systems $KAlSiO_4$–Mg_2SiO_4–SiO_2 and $KAlSiO_4$–MgO–SiO_2–CO_2 to 30 kilobars. American Journal of Science 280, 385–420.

Wendlandt, R.F., Eggler, D.H., 1980b. The origins of potassic magmas: 2. Stability of phlogopite in natural spinel lherzolite and in the $AlSiO_4$–Mg_2SiO_4–SiO_2 and $KAlSiO_4$–MgO–SiO_2–CO_2 to 30 kilobars. American Journal of Science 280, 421–4458.

Yagi, K., Matsumoto, H., 1966. Note on the leucite-bearing rocks of Leucite Hills, Wyoming, U.S.A. Journal of Faculty of Science Hokkaido University 13, 301–312.

Yoder, H.S., 1973. Melilite stability and paragenesis. Fortschritte der Mineralogie 50, 140–173.

Yoder, H.S., 1986. Potassium-rich rocks: phase analysis and heteromorphic relations. Journal of Petrology 27, 1215–1228.

Yoder, H.S., Upton, B.G.J., 1971. Diopside–Sanidine–H_2O at 5 and 10 kb. Carnegie Institute Washington Yearbook 70, 108–112.